

DOI: 10.1002/cbic.201400060

Enhancing the Efficiency and Regioselectivity of P450 Oxidation Catalysts by Unnatural Amino Acid Mutagenesis

Joshua N. Kolev, Jacqueline M. Zaengle, Rajesh Ravikumar, and Rudi Fasan^{*[a]}

The development of effective strategies for modulating the reactivity and selectivity of cytochrome P450 enzymes represents a key step toward expediting the use of these biocatalysts for synthetic applications. We have investigated the potential of unnatural amino acid mutagenesis to aid efforts in this direction. Four unnatural amino acids with diverse aromatic side chains were incorporated at 11 active-site positions of a substrate-promiscuous CYP102A1 variant. The resulting “uP450s” were then tested for their catalytic activity and regioselectivity in the oxidation of two representative substrates: a small-molecule drug and a natural product. Large shifts in regioselectivity resulted from these single mutations, and in particular, for *para*-acetyl-Phe substitutions at positions close to the heme cofactor. Screening this mini library of uP450s enabled us to

identify P450 catalysts for the selective hydroxylation of four aliphatic positions in the target substrates, including a C(sp³)–H site not oxidized by the parent enzyme. Furthermore, we discovered a general activity-enhancing effect of active-site substitutions involving the unnatural amino acid *para*-amino-Phe, which resulted in P450 catalysts capable of supporting the highest total turnover number reported to date on a complex molecule (34650). The functional changes induced by the unnatural amino acids could not be reproduced by any of the 20 natural amino acids. This study thus demonstrates that unnatural amino acid mutagenesis constitutes a promising new strategy for improving the catalytic activity and regioselectivity of P450 oxidation catalysts.

Introduction

The selective oxidation of aliphatic C–H bonds has enormous potential to facilitate the construction and manipulation of organic molecules.^[1] This transformation is notoriously challenged by the inherent strength of these chemical bonds, their widespread occurrence in organic molecules, and the higher reactivity of the oxidized products compared to the starting material. Cytochromes P450 (P450s) are a large class of heme-dependent monooxygenases that are capable of hydroxylating inactivated aromatic and aliphatic C–H bonds by using molecular oxygen under very mild conditions.^[2] As such, P450s have attracted significant interest as catalytic platforms for mediating the oxidation of organic molecules.^[3] Efforts in this area are in large part inspired by the ability of natural P450s to oxidize C–H bonds with exquisite chemo-, regio-, and stereocontrol as part, for example, of the biosynthesis of complex natural products.^[4] Achieving the same level of selectivity and catalytic efficiency with non-native substrates has, however, remained a fundamental challenge.^[5] A common strategy for affecting these properties in P450 monooxygenases is amino acid mutagenesis, by targeting the entire monooxygenase domain,^[3a,6] or by focusing on the active site,^[3i,k,m,7] or both.^[3d] For example, in combination with fingerprint-based methods for predicting P450 function, active-site mutagenesis has been

successfully used by our group to develop highly regio- and stereoselective P450 catalysts for the late-stage oxyfunctionalization of complex natural products.^[3m,7] Although large “leaps” in P450 function have typically required the combination of multiple “natural” amino acid substitutions,^[3m,7,8] we reasoned that complementary opportunities could be provided by exploring the sequence space in an orthogonal direction, that is, by expanding the number and types of amino acid residues introduced at a given position within the P450 fold.

Recent methodologies for the ribosomal incorporation of unnatural amino acids have provided a powerful and convenient tool for introducing a variety of non-proteinogenic functionalities into recombinant proteins.^[9] Over the past few years, unnatural amino acids (UAAs) have been introduced into enzymes for the purpose of studying their function^[10] or controlling their activation in a time-resolved manner.^[11] Similarly, unnatural amino acids have been used to probe the conformational properties or catalytic mechanism of P450s. For example, ¹³C-labeled *p*-methoxyphenylalanine has been introduced in CYP119 to monitor the conformational changes occurring upon substrate binding.^[12] Other groups have replaced the heme-ligating cysteine^[13] and other conserved residues^[14] in P450cam so that the role of these amino acid residues on the catalytic function of the monooxygenase can be examined. In contrast, studies on modulating the catalytic properties of enzymes by unnatural amino acid mutagenesis are scarce,^[15] and, for P450 enzymes, limited to global-substitution approaches.^[16]

The potential of unnatural amino acid mutagenesis for modulating and (ideally) improving the catalytic and selectivity

[a] J. N. Kolev, J. M. Zaengle, R. Ravikumar, Prof. R. Fasan
Department of Chemistry, University of Rochester
Hutchison Hall, Rochester, NY 14620 (USA)
E-mail: fasan@chem.rochester.edu

 Supporting information for this article is available on the WWW under <http://dx.doi.org/10.1002/cbic.201400060>.

properties of P450-based oxidation catalysts has thus remained largely unexplored. Here, we report the successful incorporation of four aromatic UAAs at multiple positions within the active site of a catalytically self-sufficient bacterial P450 (CYP102A1). The relative benefits conferred by this approach with respect to conventional mutagenesis were investigated by using two representative target substrates. Our studies demonstrate the distinctive ability of certain unnatural amino acids to alter P450 reactivity in a way that none of the natural amino acids does, thereby enabling the rapid development of P450 catalysts with greatly improved site selectivity and catalytic efficiency.

Results and Discussion

Incorporation of unnatural amino acids into a CYP102A1 variant

The long-chain fatty acid monooxygenase CYP102A1 (P450_{BM3}) from *Bacillus megaterium*^[17] was chosen as a model system for this study. CYP102A1 has provided an attractive scaffold for the development of P450-based oxidation catalysts,^[5,18] especially in view of its high activity (compared to other natural P450s) and its catalytic self-sufficiency as given by its single-component organization (i.e., heme-containing monooxygenase domain is genetically fused to a diflavin reductase^[19]). In particular, an engineered variant of CYP102A1, called 139–3,^[3a] was chosen as the parent enzyme for the incorporation of the target unnatural amino acids. Variant 139–3 contains two mutations within the active site (Val78Ala, Ala184Val) that expand the volume of the heme pocket by about 30 Å³.^[8] As a result of these mutations and nine additional ones across the heme domain (see the Supporting Information), this P450 exhibits high oxidation activity across a broad range of substrates, which include linear alkanes,^[3a] terpenes,^[8] and synthetic small molecules.^[3f]

Based on the crystal structure of this variant,^[8] 11 active-site positions were selected for substitution: Ala74, Leu75, Ala78, Phe81, Ala82, Phe87, Leu181, Val184, Leu188, Thr327, and Ala328 (Figure 1 A). The sites include residues that are located near the heme prosthetic group (e.g., 87, 328) as well as more remote positions (e.g., 184, 188). In addition, the parental residues contain different apolar side chains, ranging from aromatic (Phe) to branched (Val, Leu) and unbranched aliphatic (Ala) groups.

A wide range of unnatural amino acids have been incorporated into proteins by amber stop codon suppression and orthogonal aminoacyl-tRNA synthetase/tRNA pairs in *Escherichia coli*.^[9a] From these, four were chosen for this study, namely *para*-amino-phenylalanine (pAmF),^[20] *para*-acetyl-phenylalanine (pAcF),^[21] *O*-benzyl-tyrosine (OBnY),^[22] and 3-(2-naphthyl)alanine (NapA)^[23] (Figure 1 B). These structures contain a diverse set of aromatic side chains that differ both in overall size (e.g., pAmF and pAcF vs. OBnY and NapA) and in the nature and H-bonding properties of the functional group on the aromatic

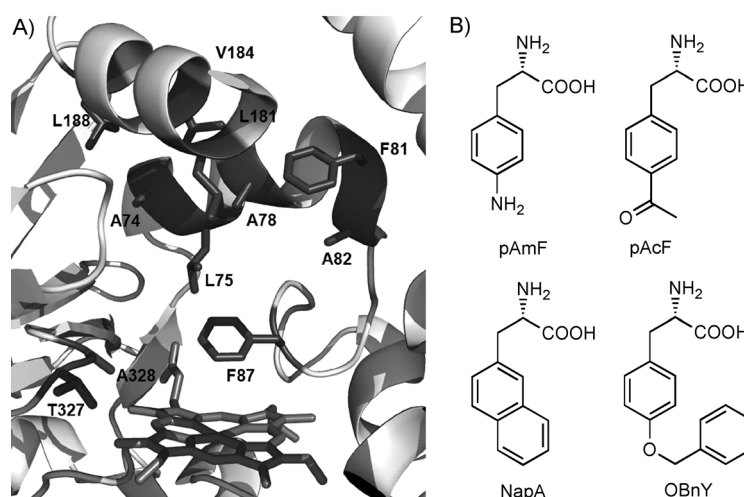


Figure 1. A) View of the active site of CYP102A1 variant 139–3 (PDB ID: 3CBD). The heme group and amino acid residues targeted for mutagenesis are displayed as stick models. B) Chemical structures of the unnatural amino acids investigated in this study (pAmF: *para*-amino-phenylalanine; pAcF: *para*-acetyl-phenylalanine; NapA: 3-(2-naphthyl)alanine; OBnY: *O*-benzyl-tyrosine).

ring (e.g., acetyl vs. amino group in pAcF and pAmF, respectively).

To allow the site-selective incorporation of these UAAs into 139–3, each of the codons for the selected active-site positions was replaced with an amber stop codon (TAG) in the gene encoding for the P450 enzyme. The corresponding enzyme variants were then expressed in *E. coli* cells containing the appropriate, engineered *Methanococcus jannaschii* tyrosyl-tRNA synthetase and cognate amber suppressor tRNA_{CUA} in the presence of the desired UAA. After expression, cells were lysed, and the amount of each of the 44 UAA-containing P450 variants (“uP450s”) was determined by CO binding assay. The specificity of incorporation for each of the aminoacyl-tRNA synthetases (aaRSs) under the applied expression conditions was confirmed through control experiments in which no UAA was added to the culture medium; these resulted in no detectable amount of recombinant P450. The expression yields were then compared to that of the parent enzyme (Figure 2).

As evidenced by these data, half of the desired uP450s (22/44) could be expressed in good to very good yields, that is, with 10 to 95% relative expression yield compared to the parent enzyme (Figure 2). Additional 12 variants could be obtained in lower but still appreciable amounts, that is, with yields ranging from 2 to 15 mg protein per liter of culture. Overall, these experiments demonstrated the feasibility of incorporating a diverse set of aromatic UAAs within the active site of a P450.

Dependence of uP450 expression yield on mutagenesis site and type of UAA

As the expression yield reflects the degree by which a mutation is tolerated,^[24] insights into the dependence of this parameter on the position targeted for mutagenesis and the nature of

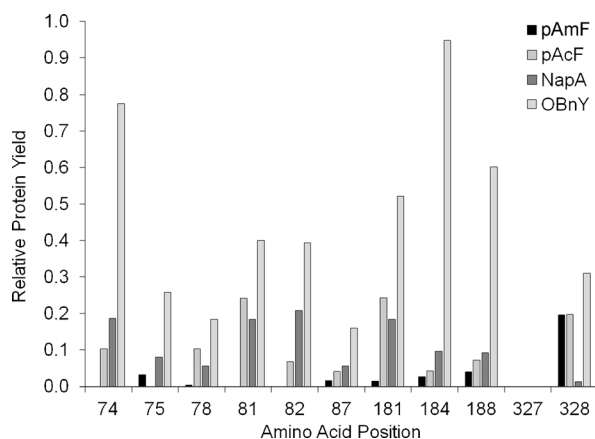


Figure 2. Relative expression yield for the uP450 variants (normalized to that of the parent enzyme, 139–3).

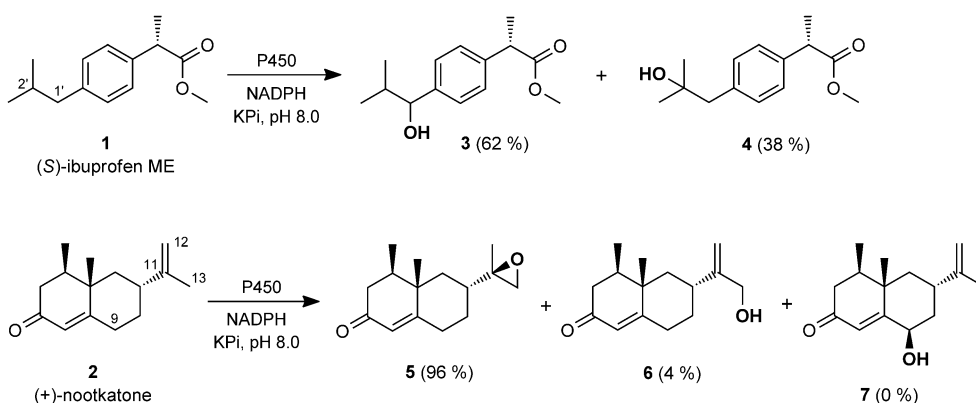
the UAA can be gained from the data in Figure 2. A prerequisite for these analyses, however, is that the expression level of the uP450 is not significantly affected by the relative incorporation efficiency of the respective aaRS. Control experiments with a reporter Yellow Fluorescent Protein showed that the poor expression levels of the pAmF-containing uP450s are due to the low activity of the pAmF-RS synthetase (Figure S1). In contrast, the amount of YFP produced with the other aaRSs was comparable, with the variation in YFP expression level being considerably lower ($SD < 15\%$, Figure S1) than the two- to tenfold differences observed for the NapA-, OBnY-, and pAcF-containing uP450s. These results indicated that the latter can be used to assess the extent by which these substitutions are tolerated by the P450 scaffold.

Accordingly, comparison of the average expression yields across all the 11 active site positions indicated that substitutions with OBnY are much better tolerated (45% av. rel. yield) than those with NapA (11%) or pAcF (11%). This trend was somewhat surprising considering the relatively large steric bulk associated with the side chain of OBnY as compared to pAcF and suggests that this feature does not critically affect the stability of the resulting uP450. All positions except Thr327 were found to be able to accommodate the incorporation of two or more UAAs. The intolerance of the 327 site to introduction of any of the UAAs is likely due a general incompatibility of this site to mutagenesis for structural reasons, as suggested by the fact that only isosteric substitutions (i.e., Thr327Val) have been reported at this site.^[18] Interestingly, no correlation was found between the nature of the parental residue and the relative tolerance of the site to UAA mutagenesis. Indeed, the average

relative expression yield (across all UAAs except pAmF) for positions occupied by phenylalanine (18%) was lower than and comparable to that for positions occupied by branched aliphatic residues (Val or Leu; 31%) and Ala (20%), respectively. Importantly, these results demonstrated that the introduction of aromatic residues of various size, as encompassed by the set of UAAs investigated here, is not restricted to positions occupied by aromatic residues (i.e., F87 and F81).

Oxidation of (*S*)-ibuprofen and (+)-nootkatone by the parent P450

A small library of uP450s was thus made available to examine the effect of UAA mutagenesis on the catalytic and selectivity properties of the enzyme. Two model substrates were selected for this purpose: (*S*)-ibuprofen methyl ester (**1**) and (+)-nootkatone (**2**, Scheme 1). These compounds have a large number of different C–H bonds (primary, secondary, tertiary, aromatic) as well as various functional groups (carbonyl, ester, olefinic group), thus making them challenging targets for selective C–H bond oxidation. In addition, they differ in size and in structural complexity, thus providing the opportunity to evaluate the effect of UAA substitutions in a small-molecule drug (**1**)



Scheme 1. Oxidation products obtained from the P450-catalyzed transformations of (*S*)-ibuprofen methyl ester and (+)-nootkatone. The product distribution of the parent P450 (139–3) is indicated in brackets.

and a natural product (**2**). Interest in the late-stage functionalization of (+)-nootkatone stems from the compound's promising activity as an antiproliferative agent in addition to its commercial value as a fragrance compound.^[25]

Oxidation of **1** with the parent enzyme 139–3 occurs with poor selectivity, producing a 62:38 mixture of the benzylic alcohol **3** and tertiary alcohol **4**, respectively (Scheme 1). On the other hand, 139–3-catalyzed transformation of **2** favors oxidation of the C11=C12 double bond to form epoxide **5** (96%) together with small amounts of the allylic alcohol **6** (4%). The chosen substrates thus provided ideal test cases to evaluate the potential of UAA mutagenesis in improving the enzyme regioselectivity, in the case of **1**, and steering such selectivity towards less activated positions (i.e., aliphatic C–H bonds), in the case of **2**.

Site selectivity of uP450s in the oxidation of the target substrates

Accordingly, the uP450 variants were screened *in vitro* for activity on these substrates by using P450 from cell lysate in the presence of a NADPH cofactor-regeneration system consisting of phosphite and a thermostable phosphite dehydrogenase.^[26] Notably, nearly all the uP450 variants (41/44) were found to exhibit measurable oxidation activity on both **1** and **2** (Table S2). These include the variants whose concentration was below the detection limit for the CO binding assay (e.g., pAmF variants and Thr327UAA variants, Figure 2). Not surprisingly, the substrate conversion ratio varied considerably as a result of the different reactivity of the enzymes as well as their difference in concentration in the lysate.

As shown by the data in Table S2, incorporation of the four non-proteinogenic amino acids at the various active-site positions altered the product distribution for the oxidation of **1** and/or **2** to a greater or lesser degree. Interestingly, a new oxidation product of **2** was also observed, which was determined to correspond to (9*R*)-hydroxynootkatone (**7**, Scheme 1). Inspection of these results allowed for a first general evaluation of the relative effect of each type of UAA on the enzyme site-selectivity. Of the 88 possible uP450/substrate combinations, 31 % displayed at least a moderate change in regioselectivity, with this effect being fairly evenly distributed across all unnatural amino acids except pAmF (Figure 3). With the more stringent threshold of >30% variation in site selectivity, this number is reduced to 15 uP450s. Among these, the OBnY- and pAcF-containing variants are more largely represented than the NapA- and pAmF-containing uP450s (Figure 3); this indicates that substitutions with the first two UAAs generally have a larger effect on the enzyme site selectivity. Finally, analysis of the variants with the largest variation in product distribution (>50%) revealed that mutagenesis with pAcF has the largest potential to cause dramatic changes in the regioselectivity of oxidation.

The dependence of these changes on the substrate, the site targeted for mutagenesis, and the nature of the parental resi-

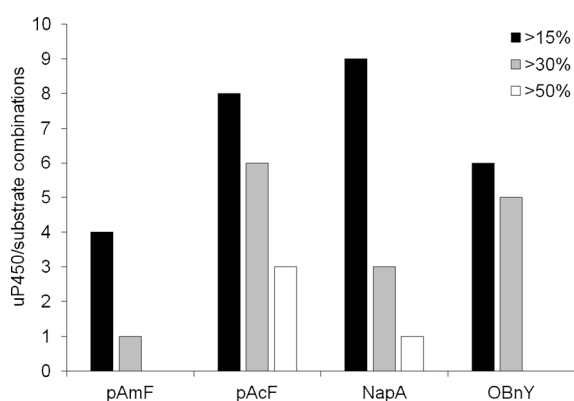


Figure 3. Distribution of uP450/substrate (**1** or **2**) combinations showing more than 15, 30, or 50% change in site selectivity (vs. parent enzyme), subdivided according to the type of unnatural amino acid incorporated into the P450.

due was also examined. On average, a larger number of important shifts in regioselectivity (>30% variation vs. parent enzyme) were observed in the context of (*S*)-ibuprofen methyl ester (**1**) than for (+)-nootkatone (**2**; 10 vs. 6, Table S2); this might reflect the fact that altering the orientation of a flatter substrate (**1**) within the enzyme active site is easier than for a bulkier one (**2**).

Furthermore, the largest regioselectivity shifts were observed for substitutions involving amino acid residues whose β -carbon is within 12–13 Å from the heme iron (i.e., positions 78, 82, 328, Figure 1 A); this supports our previously advanced hypothesis that first-sphere active-site residues are preferred targets for modulating this property in P450s.^[3m] Finally, the following order of dependence of the regioselectivity changes on the nature of the parental residue emerged (Table S2): Ala (largest changes) > Val/Leu \gg Phe (smallest changes). This trend can be rationalized on the basis of the structural difference between the side chain group of the UAA and that of the substituted amino acid in the parental sequence.

Other interesting observations could be made from comparison of variants incorporating different unnatural amino acids at the same position of the active site (Table 1). For example, substitution of position 78 and 82 (Figure 1) with any of the four UAAs resulted in significantly different product profiles for the oxidation of **2**, whereas little or no change in regioselectivity was observed for these variants in the oxidation of **1** (entries 2–9, Table 1). Conversely, introduction of either OBnY or pAcF at position 181 was found to induce a large shift in the regioselectivity of oxidation with **1**, whereas both variants exhibited a parent-like product profile in the presence of **2**. Thus, beyond the general trends discussed above, these results illustrate the abilities of the UAAs considered here to induce unique changes in regioselectivity, as dependent on the structure of substrate as well as the site targeted for mutagenesis.

Characterization of the most selective uP450 variants

The above experiments revealed that a number of uP450s exhibit a significant improvement in regioselectivity over the parent enzyme. Accordingly, the most selective variants, namely Ala78pAcF, Ala82pAcF, and Ala328NapA, were isolated and further characterized in purified form (Table 2).

As shown in Scheme 1, the parent enzyme is unselective in the oxidation of **1**, producing a 62:38 mixture of the C1' and C2' hydroxylation products. From the small library of uP450s, two variants that exhibit much higher regioselectivity toward each of these aliphatic sites could be isolated. In particular, variant Ala78pAcF was found to hydroxylate the C1' benzylic position with 88% regioselectivity, whereas variant Ala328NapA produces the hydroxylated product **4** with 95% regioselectivity (Table 2). Similarly, two variants could be identified that exhibit a large shift in selectivity toward C–H hydroxylation over epoxidation in the presence of **2**. Variant Ala82pAcF shows much higher regioselectivity for hydroxylation of the C13 position than 139–3, forming **6** with 62% selectivity (4% for the parent enzyme). On the other hand, variant Ala78pAcF catalyzes the formation of **7**, which is not produced by the parent enzyme,

Table 1. Effect of UAA substitutions on the regioselectivity of oxidation of (S)-ibuprofen methyl ester (**1**) and (+)-nootkatone (**2**).

	Position	UAA	Product [%]				
			3 ^[a]	4 ^[a]	5 ^[b]	6 ^[b]	7 ^[b]
1	parent P450		62	38	96	4	0
2		pAmF	68	32	91	9	0
3	78	pAcF	87	13	32	0	68
4		NapA	79	21	79	6	15
5		OBnY	65	35	64	0	36
6		pAmF	73	27	79	21	0
7	82	pAcF	72	28	38	62	0
8		NapA	78	22	51	41	8
9		OBnY	67	33	57	22	21
10		pAmF	60	40	96	4	0
11	181	pAcF	30	70	79	4	17
12		NapA	53	47	81	4	15
13		OBnY	15	85	93	7	0

[a] From (S)-ibuprofen methyl ester (**1**). [b] From (+)-nootkatone (**2**).

with high regioselectivity (73%) and absolute stereoselectivity (no formation of the corresponding epimer (9S)-hydroxynootkatone). Consistent with the general trend emerging from our previous analysis (Figure 3), three out of the four most selective transformations are mediated by pAcF-containing uP450s. These results thus confirm that this UAA had the highest potential among those tested to affect the site selectivity in a P450.

139–3 catalyzes the oxidation of the target substrates with good efficiency, supporting nearly 8000 total turnovers (TTN) with **1** and about 7000 TTN with **2** (Table 2) with initial product formation rates of 420 and 175 min⁻¹, respectively. Comparison of the TTN values and product formation rates for the uP450 variants show that both of these properties are affected by the UAA substitutions (Table 2). In each case (i.e., for Ala78pAcF, Ala82pAcF and Ala328NapA), the improvement in regioselectivity in the presence of **1** and/or **2** is accompanied by a three- to tenfold reduction in TTN. Measurement of the coupling effi-

ciency for these variants showed that, in most cases, the decrease in TTN corresponds to a reduction in coupling efficiency, which could lead to a faster inactivation of the enzyme during catalysis. For the Ala328NapA and Ala82pAcF variants, the improvement in regioselectivity in the transformation of **1** and **2**, respectively, is also associated with a decrease in the oxidation rate (Table 2). Interestingly, the data corresponding to these uP450s also indicate that the effect on TTN and catalytic rate is more prominent with the substrate oxidized with higher selectivity, thus indicating a general trade-off between these properties as we observed with P450 catalysts evolved by conventional mutagenesis.^[3m,7]

These trends notwithstanding, the catalytic efficiency of these selective P450 variants remains elevated (i.e., 700–2500 total turnovers) and thus well suited for synthetic applications, as established by the successful isolation of **6** and **7** from large-scale reactions (40 mg (+)-nootkatone) with Ala82pAcF (0.13 mol%) and Ala78pAcF (0.05 mol%), respectively (see the Experimental Section). Most importantly, these results showed that by screening a minimal library of UAA-containing P450s (44), selective catalysts could be rapidly obtained for oxyfunctionalization at a total of four aliphatic C–H sites in a small-molecule drug and a natural product, including one position not accessible to the parent enzyme.

Activity-enhancing effect of pAmF mutations

During the initial screening of the uP450 variants from cell lysate, we noticed that the substrate conversion yields ob-

Table 2. Catalytic properties of selected P450 variants in the oxidation of (S)-ibuprofen methyl ester (**1**) and (+)-nootkatone (**2**).

Variant	(S)-Ibuprofen methyl ester (1)							(+)–Nootkatone (2)						
	3	4	TTN ^[a]	Relative activity	Initial rates ^[b]	Coupling efficiency ^[c]	5	6	7	TTN ^[a]	Relative activity	Initial rates ^[b]	Coupling efficiency ^[c]	
parent P450	62%	38%	7950 ± 860	1.0	420	48%	96%	4%	0%	6980 ± 130	1.0	175	11%	
Ala78pAcF	88%	12%	2400 ± 250	0.3	405	31%	27%	0%	73%	1760 ± 70	0.3	170	13%	
Ala82pAcF	75%	25%	1100 ± 130	0.1	89	6%	38%	62%	0%	720 ± 70	0.1	36	8%	
Ala328NapA	5%	95%	675 ± 10	0.1	12	4%	75%	25%	0%	2460 ± 70	0.4	38	6%	
Leu75pAmF	14%	86%	11120 ± 270	1.4	200	25%	93%	7%	0%	34650 ± 1620	5.0	685	43%	
Phe81pAmF	34%	66%	12310 ± 620	1.5	550	41%	93%	7%	0%	16120 ± 400	2.3	455	24%	
Leu188pAmF	65%	35%	21320 ± 1250	2.7	1220	68%	97%	3%	0%	15470 ± 1040	2.2	515	27%	
Leu75Tyr	53%	47%	1330 ± 180	0.2	450	22%	90%	10%	0%	11640 ± 290	1.7	1650	84%	
Phe81Tyr	24%	76%	1620 ± 80	0.2	380	24%	93%	7%	0%	9460 ± 380	1.4	740	40%	
Leu188Tyr	60%	40%	3220 ± 220	0.4	1260	26%	96%	4%	0%	10410 ± 260	1.5	715	11%	

[a] Reaction conditions: 0.002–0.01 mol% P450, 1 mM substrate, cofactor regeneration system (2 μM PTDH, 100 μM NADP⁺, 50 mM sodium phosphite) in phosphate buffer (50 mM, pH 8.0), 16 h. [b] Expressed as moles of product formed per mole of P450 per minute. SD < 15%. [c] Ratio between rates of product formation and NADPH consumption in the presence of the substrate.

tained with the pAmF-containing P450s were comparable to those observed in the presence of other uP450s. As the pAmF-containing variants are expressed at much lower levels (Figure 2), these results implied that these enzymes are capable of supporting higher substrate turnover numbers. To investigate this aspect, the most promising variants (Leu75pAmF, Phe81pAmF, and Leu188pAmF) were expressed and further characterized in purified form. They were indeed found to catalyze the oxidation of **1** and **2** with much higher efficiency not only than the previously characterized uP450s but also than the parent enzyme, supporting two to five times higher TTN than the latter (Table 2). A general increase in the product formation rate, ranging from two- to fourfold, was also observed. Notably, the total turnover numbers measured for Leu75pAmF with **2** (34 650) corresponds to the highest TTN value reported for an engineered P450 on a complex molecule.^[5] Moreover, the catalytic rate for Leu188pAmF on **1** (1220 min^{-1}) approaches that exhibited by wild-type CYP102A1 on fatty acid substrates (e.g., 1680 min^{-1} with laurate^[27]), which themselves remain among the highest ones among known natural P450s.

The unanticipated beneficial effect of pAmF substitutions on the catalytic efficiency of the monooxygenase called for further investigations to examine the basis of this phenomenon. Analysis of the product distribution for the pAmF-containing variants with both **1** and **2** showed no significant changes from that of the parent enzyme in nearly all cases (5/6, Table 2), thus suggesting that these activity enhancements are not linked to a change in the binding mode of the substrate upon oxidation. Furthermore, inspection of the enzyme crystal structure revealed that, unlike the regioselectivity-altering mutations, these activity-enhancing substitutions are not restricted to residues located close to the heme cofactor. Indeed, these sites included Leu188, whose β -carbon lies rather far ($\sim 20 \text{ \AA}$) from the heme iron center (Figure 1).

Given the H-bonding capabilities of the aromatic amino group in pAmF and the presence of various H-bond donor/acceptor groups in both **1** and **2**, we wondered whether the improved catalytic efficiency of the pAmF-containing variants could stem from an increase in enzyme affinity for the substrate. To investigate this aspect, heme spin-shift experiments were carried out. Whereas **1** failed to induce a detectable spectral shift of the Soret band in the presence of both 139–3 and the pAmF variants, a significant shift of the heme spin state (from 20 to 60%) could be observed upon addition of **2** to these P450s (Figure 4). Calculation of the equilibrium dissociation constants indicated that the affinities of the pAmF variants for **2** are relatively high, with the corresponding K_D values ranging from 16 to $32 \mu\text{M}$ (Figure 4). However, these values were found to be comparable to that of the parent enzyme ($K_D = 14 \mu\text{M}$); this suggests that the pAmF substitutions do not significantly improve the binding affinity for this substrate. Moreover, these experiments show no apparent correlation between the extent of **2**-induced heme spin shift and the difference in catalytic performance for these P450s (Figure 4).

In contrast, measurement of the coupling efficiency revealed a good correlation between this parameter and improved catalytic properties of these variants across both substrates

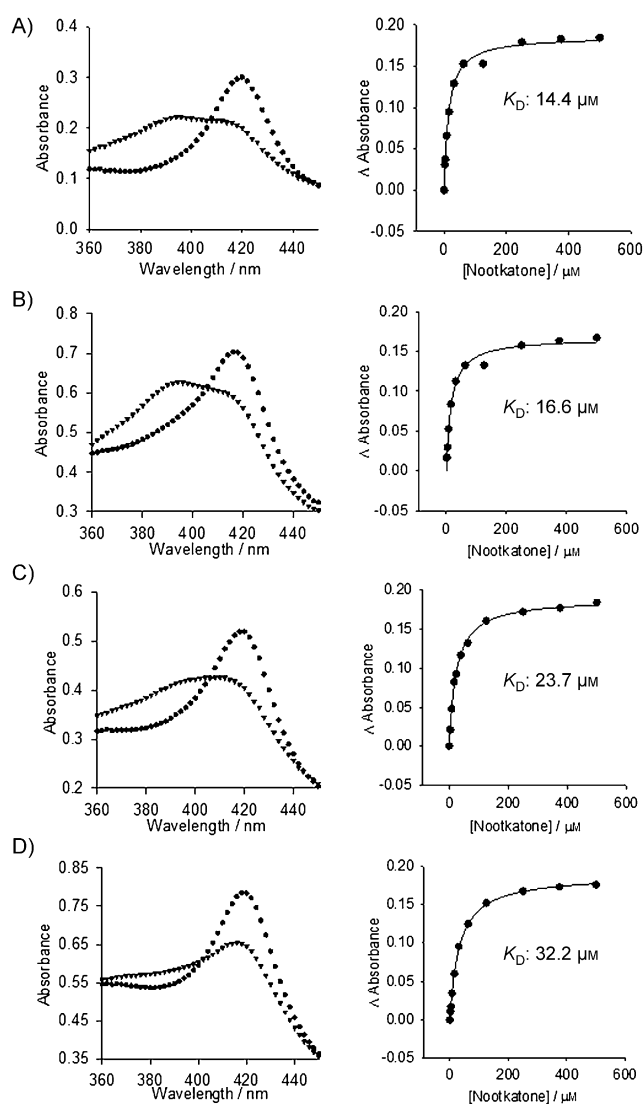


Figure 4. Heme spin-shift experiments with the pAmF-substituted P450s: A) parent P450, B) Leu75pAmF, C) Phe81pAmF, and D) Leu188pAmF. Left: Electronic absorption spectrum before (●) and after (▼) addition of (+)-nootkatone at saturating concentration (0.5 mM). Right: Representative plots of the enzyme heme spin shift at varying (+)-nootkatone concentration. The equilibrium dissociation constants (K_D) as calculated by fitting the experimental data (●) to a non-cooperative 1:1 binding model equation (—), are indicated.

(Table 2). With **2**, both the product formation rate and TTN values were found to increase almost linearly with the increase in coupling efficiency (Table 2). Although a less direct correlation is seen with **1**, also in this case the fastest and most efficient variant, Leu188pAmF, is characterized by the highest coupling efficiency (Table 2).

Tyrosine versus pAmF substitutions

Among the natural amino acids, tyrosine is most closely related to pAmF from a structural standpoint; this raised the question of whether the beneficial effects obtained with this non-proteinogenic amino acid could be reproduced by tyrosine.

The 139–3-based single mutants Leu75Tyr, Phe81Tyr, and Leu188Tyr were prepared and characterized (Table 2). Interestingly, similarly to the pAmF variants, tyrosine substitution at each of these sites was found to induce a significant increase in catalytic rate with both **1** (two- to threefold) and **2** (four- to ninefold) relative to the parent P450. These variants also showed, for the most part, parent-like regioselectivity with both **1** and **2** as well as parent-like binding affinity for **2** ($K_D = 14\text{--}48\ \mu\text{M}$, Figure S2), as observed for the pAmF-incorporating counterparts. In spite of these similar features, the pAmF variants remained significantly superior oxidation catalysts (in terms of total turnover numbers) to their Tyr-substituted counterparts. This general trend is apparent with **2**, for example, with Leu75pAmF supporting nearly threefold higher total turnovers than Leu75Tyr (34650 vs. 11640 TTN), but it is particularly striking in the case of **1** (Table 2). With **1**, the turnover numbers supported by the pAmF variants are up to seven times higher than those obtained with the corresponding Tyr-containing P450s.

Altogether, the above studies showed the distinct advantage of pAmF substitutions in enhancing the catalytic efficiency of P450s. This beneficial effect apparently stems from their ability to promote a more efficient oxidation of the substrate by the enzyme, as suggested by the correlation between TTN and coupling efficiency discussed earlier. This phenomenon has been linked to a more favorable enzyme–substrate interaction.^[8,28] However, our binding studies (i.e., K_D values, heme spin shift assays) with both the pAmF variants and their Tyr-substituted counterparts do not support this scenario. As an alternative hypothesis, the pAmF substitutions could suppress unproductive, ROS-producing pathways during the P450 catalytic cycle, slowing inactivation of the enzyme and thus higher total turnover numbers. How this effect is exerted by pAmF substitutions at multiple sites within the enzyme active site (i.e., 75, 81, 188) and across structurally different substrates remains unclear.

Comparison with natural amino acid mutagenesis

Based on the data accumulated at this point, it became apparent that pAcF and pAmF have a distinctive ability to induce dramatic changes in the regioselectivity and catalytic efficiency, respectively, of a P450 enzyme. To examine whether these effects could have been achieved with any of the natural amino acids, two of the targeted active-site positions, Ala75 and Leu78, were subjected to site-saturation mutagenesis. Position 78 was chosen because its substitution with pAcF causes one of the largest regioselectivity shifts observed in this study (0 → 73% for the C9 position in **2**), leading to a variant capable of hydroxylating a C–H bond not accessible to the parent enzyme with high regio- and stereoselectivity. Position 75 was chosen as its substitution with pAmF results in the most efficient P450 catalyst identified here (> 34600 TTN with **2**). In addition, Leu75pAmF also exhibits greatly improved regioselectivity toward hydroxylation of C2' in **1** compared to 139–3 (38 → 86%, Table 2).

Accordingly, two site-saturation libraries (75NNK and 78NNK) were constructed by mutating positions 75 and 78 in 139–3 using the degenerate codon NNK (any base in first and second position; G or T in third position). The functional members from each library (threefold oversampling) were then identified by high-throughput fingerprinting,^[29] followed by analysis of their oxidation activity on **1** and **2** through in vitro reactions. Analysis of the reactions with **2** showed that all the variants from these libraries exhibit parent-like regioselectivity. In addition, the most active variant within this pool of engineered P450s was estimated to support at most a twofold higher TTN than the parent enzyme. Thus, none of the 75 or 78 site-saturation variants could reproduce the catalytic or site-selectivity features of Leu75pAmF or Leu78pAcF, respectively. Similarly, none of the P450 variants from the 75NNK library could reproduce the large regioselectivity shift displayed by Leu75pAmF with **1**. Indeed, the highest C2' selectivity observed among these variants was 71% (vs. 86% for Leu75pAmF), with the minor product (29%) being **3**. Altogether, these experiments along with the studies on the Tyr mutants, showed that none of the amino acid mutations accessible through conventional mutagenesis could reproduce the largest functional changes imparted by the pAcF and pAmF substitutions.

Conclusions

We have investigated the site-selective incorporation of various unnatural amino acids into a cytochrome P450 monooxygenase and the effect of these modifications on its selectivity and reactivity properties. Our results show that different aromatic unnatural amino acids, including two comprising large (naphthyl) and extended (benzyloxybenzene) side chains, can be accommodated at many positions (10/11) within the active site of the enzyme. Importantly, by screening this small library of singly substituted uP450s, selective P450 catalysts for the hydroxylation of four aliphatic C–H sites in a drug molecule and a natural product could be rapidly identified. A particularly interesting trend emerging from these studies is the inherent potential of pAcF substitutions, in particular at the level of “first-sphere” active-site positions, to alter the site selectivity of a P450 monooxygenase. Another relevant finding is the general activity-enhancing effect of active-site substitutions with pAmF, which resulted in P450 catalysts capable of supporting among the highest numbers of total turnovers reported for an engineered P450. These findings are expected to have implications in the design and development of improved P450-based oxidation catalysts. They also lay the ground for future studies aimed, for example, at elucidating the mechanism underlying the activity-enhancing effects of pAmF substitutions and further examining the generality of these effects (e.g., in other P450 systems). It will be also interesting to determine whether the effects of pAmF and pAcF substitution can be combined. Importantly, our studies showed that the functional changes induced by these non-proteinogenic amino acids could not be recapitulated by any of the natural amino acids. As such, this work demonstrates that unnatural mutagenesis constitutes

a promising strategy for modulating and enhancing the selectivity and catalytic efficiency of P450-based oxidation catalysts.

Experimental Section

Reagents and analytical methods: Chemical reagents and solvents were purchased from Sigma–Aldrich, AlfaAesar, Chem-Impex, and Fluka. Silica gel chromatography purifications were carried out by using AMD silica gel 60 230–400 mesh. 1D and 2D NMR experiments were carried out on a Avance 500 MHz spectrometer (Bruker). Data for ^1H and ^{13}C NMR spectra are reported (δ ppm) against tetramethylsilane. Mass spectra were collected by direct infusion on a LTQ Velos ESI/ion-trap mass spectrometer (Thermo Scientific). Gas chromatography analyses were carried out on a Shimadzu GC2010 equipped with a FID detector and a Restek RTX-5 column (15 m \times 0.25 mm \times 0.25 μm film). Separation methods: (S)-ibuprofen methyl ester (**1**): 260 °C inlet, 260 °C detector, 120 °C oven, 17 °C min $^{-1}$ ramp to 150 °C, 10 °C min $^{-1}$ ramp to 240 °C, and 240 °C for 1 min; (+)-Nootkatone (**2**): 260 °C inlet, 260 °C detector, 120 °C oven, 12 °C min $^{-1}$ ramp to 220 °C, 220 °C for 1 min, 20 °C min $^{-1}$ ramp to 250 °C, and 250 °C for 1 min.

Synthesis of (S)-ibuprofen methyl ester (1**):** (S)-Ibuprofen (341 mg, 1.65 mmol) and sulfuric acid (100 μL) in methanol (20 mL) were heated under reflux for 16 h. Saturated sodium bicarbonate (10 mL) was added, then the methanol was removed by evaporation under reduced pressure. The solution was extracted with CH_2Cl_2 (3 \times 5 mL). The organic layers were dried over sodium sulfate and evaporated to give a colorless oil, which was purified by flash chromatography (hexanes/ethyl acetate 8:1) to yield **1** (245 mg, 67%). ^1H NMR (500 MHz, CDCl_3): δ = 0.90 (d, J = 6.7 Hz, 6H), 1.49 (d, J = 7.2 Hz, 3H), 1.85 (sept, J = 6.9 Hz, 1H), 2.45 (d, J = 6.9 Hz, 2H), 3.66 (s, 1H), 3.70 (q, J = 7.2 Hz, 1H), 7.09 (d, J = 7.7 Hz, 2H), 7.20 ppm (d, J = 8.1 Hz, 2H); ^{13}C NMR (125 MHz, CDCl_3): δ = 18.65, 22.42, 30.18, 45.04, 51.98, 127.13, 129.356, 137.75, 140.56, 175.23 ppm; MS (ESI) calcd for $\text{C}_{14}\text{H}_{20}\text{O}_2$ $[\text{M}+\text{H}]^+$ m/z : 221.15; found: 221.20.

Synthesis of the unnatural amino acids: pAcF was synthesized from acetophenone as described by Satyanarayana et al.^[30] OBnY was prepared from L-tyrosine according to the procedures reported by Stokes et al.^[22] NMR and MS data for these compounds were consistent with those reported. pAmF and NapA were purchased from AlfaAesar and Sigma–Aldrich, respectively.

Cloning and plasmid construction: A pCWori-based vector encoding for the CYP102A1 variant 139–3^[3a] was kindly provided by the group of Frances Arnold (Caltech). Compared to wild-type CYP102A1, 139–3 contains the following mutations: V78A, H138Y, T175I, V178I, A184V, H236Q, E252G, R255S, A290V, A295T, and L353V. Vectors encoding for the amber stop codon-containing P450 variants were prepared by using pCWori_139–3 as a template, primers BamHI_2_fwd (5'-GGAAA CAGGA TCCAT CGATG C-3') and SacI_2_rev (5'-AATAT CGAGC TCGTA GTTTG TATGA TC-3') as megaprimers, and the oligonucleotides given in Table S1 as mutagenizing primers. The target gene products (1.5 kb) were prepared by PCR overlap extension mutagenesis, digested with BamHI and SacI restriction enzymes, and ligated to BamHI/SacI doubly digested pCWori vector. The plasmid pEVOL_pAcF encoding for the engineered *M. jannaschii* tRNA_{CUA} and aaRS for amber codon suppression with pAcF was kindly provided by the group of Peter G. Schultz (The Scripps Research Institute). Plasmids for the expression of pAmF-RS,^[20] NapA-RS,^[23] and OBnY-RS (=Bpa-RS(V164A)^[22]) were prepared by introducing the following mutations into both

copies of the aaRS gene in the pEVOL_pAcF vector: pAmF-RS: Y32T, E107T, D158P, I159L, L162A; NapA-RS: Y32L, D158P, I159A, L162Q, A167V; OBnY-RS: Y32G, E107P, D158T, I159S, V164A. The plasmid vector for the expression of Yellow Fluorescent Protein containing an amber stop codon after the initial Met residue was prepared by PCR amplification of the YFP gene from pEYFP-N1 (BD Biosciences) by using primers YFP(stop)_for (5'-GGTTC CATAT GGGTT AGGTG AGCAA GGGCG AGGAG C-3') and YFP_(XhoI)_rev (5'-CGTTG CTCGA GCTTG TACAG CTCGT CCATG CC-3'). The PCR product (0.7 kb) was then cloned into pET22b(+) (Novagen) by using NdeI and XhoI to give pET22_YFP(stop) plasmid. The identity of the cloned constructs was confirmed by DNA sequencing.

Protein expression and purification: The UAA-containing P450s were expressed in *E. coli* DH5 α cells cotransformed with the pCWori-based vector encoding for the P450 and the appropriate pEVOL vector encoding for the orthogonal tRNA_{CUA}/aaRS pair. Overnight cultures in lysogeny broth (LB) containing ampicillin (100 mg L $^{-1}$) and chloramphenicol (26 mg L $^{-1}$) were used to inoculate M9 medium containing ampicillin (50 mg L $^{-1}$) and chloramphenicol (26 mg L $^{-1}$) supplemented with the appropriate UAA (2 mM). At OD₆₀₀ = 0.6, protein expression was induced with 0.05% arabinose, isopropyl- β -D-thiogalactopyranoside (IPTG; 0.5 mM), and δ -aminolevulinic acid (0.3 mM), followed by incubation for 24 h at 27 °C. For the initial screening of the uP450s, the proteins were expressed in 15 mL cultures, followed by lysis (0.8 mg mL $^{-1}$ lysozyme, 4 U mL $^{-1}$ deoxyribonuclease I, 10 mM MgCl₂, 50 mM phosphate buffer, pH 8.0) and clarification of the cell lysate by centrifugation (3500g, 20 min, 4 °C). For the characterization studies, selected uP450s were expressed from 0.5 L cultures and purified by ion-exchange chromatography, as described.^[29] P450 concentration was determined from CO binding difference spectra ($\epsilon_{450-500}$ = 91 000 m $^{-1}$ cm $^{-1}$). Phosphite dehydrogenase (PTDH) was expressed and purified as described previously.^[29]

YFP screen: *E. coli* BL21(DE3) cells were cotransformed with the pET22_YFP(stop) plasmid and the pEVOL plasmid encoding for the appropriate aminoacyl-tRNA synthetase, and then grown in LB containing ampicillin (50 mg L $^{-1}$) and chloramphenicol (26 mg L $^{-1}$) at 37 °C overnight. The overnight cultures were used to inoculate 96-deep well plates containing M9 medium. At an OD₆₀₀ of 0.6, cell cultures were induced by adding arabinose (0.06% m/v), IPTG (0.2 mM), and the appropriate unnatural amino acid (1 mM for L isomer). After overnight growth at 27 °C, the cell cultures were diluted (1:1) with phosphate buffer (50 mM, 150 mM NaCl, pH 7.5), and the fluorescence intensity (λ_{ex} = 514 nm; λ_{em} = 527 nm) was determined by using a Tecan Infinite 1000 plate reader. Cell cultures containing no unnatural amino acid were included as controls. Each sample was measured in quadruplicate.

Synthesis of 13-hydroxynootkatone (6**):** Purified P450 variant Ala82pAcF (1.25 μM ; 0.13 mol%) was dissolved in phosphate buffer (183 mL, 50 mM, pH 8.0) in the presence of (+)-nootkatone (40 mg, 1.0 mM), PTDH (2 μM), NADP $^+$ (150 μM), and sodium phosphite (50 mM). The reaction mixture was stirred for 12 h at room temperature. The crude product was extracted with CH_2Cl_2 (3 \times 30 mL). The collected organic layers were dried with sodium sulfate, concentrated under vacuum, and purified by flash chromatography (0–50% ethylacetate in hexanes) to afford **6** (22 mg, 51%) and **5** (12 mg, 29%).

13-Hydroxynootkatone (6**):** ^1H NMR (500 MHz, CDCl_3): δ = 0.95 (d, J = 7.0 Hz, 3H), 1.11 (s, 1H), 1.15 (t, J = 13.0 Hz, 1H), 1.37, (dq, J = 3.6, 13.4 Hz, 1H), 1.93–2.06 (m, 3H), 2.19–2.33 (m, 2H), 2.34–2.47 (m, 2H), 2.52 (ddt, J = 1.9, 5.2, 14.7 Hz, 1H), 4.14 (s, 2H), 4.90 (s, 1H),

5.08 (s, 1H), 5.76 ppm (s, 1H); ^{13}C NMR (125 MHz, CDCl_3): δ = 14.91, 16.81, 32.09, 33.08, 35.98, 39.43, 40.40, 42.04, 44.39, 65.23, 109.08, 124.77, 152.57, 170.27, 199.67 ppm; MS (ESI) calcd for $\text{C}_{15}\text{H}_{22}\text{O}_2$: m/z : 235.16 $[\text{M}+\text{H}]^+$; found: 235.2.

Nootkatone-(11R),12-epoxide (5): ^1H NMR (500 MHz, CDCl_3): δ = 0.98 (d, J = 6.8 Hz, 3H), 1.07 (s, 3H), 1.22 (t, J = 12.8 Hz, 1H), 1.24 (s, 3H), 1.55–1.67 (m, 1H), 1.85–1.93 (m, 1H), 1.95–2.09 (m, 2H), 2.19–2.32 (m, 2H), 2.33–2.40 (m, 1H), 2.45 (dt, J = 4.9, 13.9 Hz, 1H), 2.59 (d, J = 4.9 Hz, 1H), 2.65 (d, J = 4.9 Hz, 1H), 5.76 ppm (s, 1H); ^{13}C NMR (125 MHz, CDCl_3): δ = 14.93, 16.77, 17.77, 28.81, 32.46, 39.01, 39.63, 40.35, 40.54, 42.05, 53.67, 58.94, 124.90, 169.88, 199.51 ppm; MS (ESI) calcd for $\text{C}_{15}\text{H}_{22}\text{O}_2$: m/z : 235.16 $[\text{M}+\text{H}]^+$; found: 235.5. The stereochemistry of the C11 carbon atom was assigned based on comparison of NMR data with the reported values for the 11 R ^[25] and 11 S ^[31] epimers.

Synthesis of (9R)-hydroxy-nootkatone (7): Purified P450 variant Ala78pAcF (0.5 μM , 0.05 mol%) was dissolved in phosphate buffer (183 mL, 50 mM, pH 8.0) in the presence of (+)-nootkatone (40 mg, 1.0 mM), PTDH (2 μM), NADP^+ (150 μM), and sodium phosphite (50 mM). The reaction mixture was stirred for 12 h at room temperature. The crude product was extracted with CH_2Cl_2 (3 \times 30 mL). The collected organic layers were dried with sodium sulfate, concentrated under vacuum, and purified by flash chromatography (0–50% ethylacetate in hexanes) to afford **7** (23 mg, 54%). ^1H NMR (500 MHz, CDCl_3): δ = 0.95 (d, J = 6.9 Hz, 3H), 1.09 (t, J = 13.5 Hz, 1H), 1.31 (s, 3H), 1.53 (dq, J = 2.6, 13.7 Hz, 1H), 1.76 (s, 3H), 1.93–2.11 (m, 4H), 2.22–2.39 (m, 2H), 2.78 (tt, J = 2.9, 12.6 Hz, 1H), 4.46 (t, J = 2.8 Hz, 1H), 4.76 (d, J = 12.9 Hz, 2H), 5.86 ppm (s, 1H); ^{13}C NMR (125 MHz, CDCl_3): δ = 14.54, 18.12, 20.97, 34.00, 37.92, 38.81, 41.21, 42.34, 43.67, 73.36, 109.39, 127.20, 148.91, 168.30, 200.55 ppm; MS (ESI) calcd for $\text{C}_{15}\text{H}_{22}\text{O}_2$: m/z : 235.16 $[\text{M}+\text{H}]^+$; found: 235.20. The stereochemistry of the C9 carbon was assigned based on comparison of NMR data ($^3J_{9,10}$ = 2.80 Hz) with those of analogous compounds (i.e., (9R)-hydroxy-11,12-didehydronootkatone;^[29] $^3J_{9,10}$ = 2.7, 3.0 Hz).

Total turnover numbers and regioselectivity of P450 variants: Analytical-scale reactions (1 mL) were carried out by using P450 (0.02–1 μM), substrate (1 mM), PTDH (2 μM), NADP^+ (100 μM), and sodium phosphite (50 mM) in phosphate buffer (50 mM, pH 8.0). The P450 variants described in Table 2 were characterized in purified form, whereas those described in Tables 1 and S1 were characterized directly from cell lysates. After 12 h at room temperature, the reaction mixtures were added with guaiacol (500 μM) as internal standard, extracted with CH_2Cl_2 , and analyzed by gas chromatography. TTN values were calculated based on the total amount of oxidation products as quantified from calibration curves. Mean and standard deviation values reported for P450 variants in Table 2 were calculated from experiments performed at least in triplicate.

Measurement of catalytic rate, coupling efficiency, and substrate binding affinity: Initial product formation rates were measured from 1 mL scale reactions containing substrate (0.5 mM), purified P450 (0.02–0.5 μM), and NADPH (2 mM) in phosphate buffer (50 mM, pH 8.0) at room temperature. After 30 s, the samples and guaiacol (500 μM) were added, and the mixture was extracted with CH_2Cl_2 . Cofactor oxidation rate in the presence of substrate was measured by monitoring NADPH depletion at 340 nm ($\epsilon_{450-500}$ = 6.22 $\text{mm}^{-1}\text{cm}^{-1}$) by using purified P450 (0.02–0.5 μM), substrate (0.5 mM), and NADPH (200 μM). Coupling efficiency was calculated from the ratio between the initial product formation rate and the initial NADPH oxidation rate. Reported mean and standard deviation values were calculated from experiments performed at least in

triplicate. Binding experiments were performed with purified P450 (3 μM) in phosphate buffer (50 mM, pH 8.0) and various concentrations (2–500 μM) of the (+)-nootkatone.

Acknowledgements

This work was supported by the National Institutes of Health R01 grant GM098628 awarded to R.F. MS instrumentation was supported by the National Science Foundation grant CHE-0946653. J.N.K. acknowledges support from the U.S. Department of Education GAANN program (P200A120011-13). J.M.Z. and R.R. are grateful to the NFS REU program for financial support.

Keywords: cytochromes • oxidation • protein engineering • terpenes • unnatural amino acids

- [1] a) T. Newhouse, P. S. Baran, *Angew. Chem. Int. Ed.* **2011**, *50*, 3362–3374; *Angew. Chem.* **2011**, *123*, 3422–3435; b) S. R. Neufeldt, M. S. Sanford, *Acc. Chem. Res.* **2012**, *45*, 936–946; c) T. Brückl, R. D. Baxter, Y. Ishihara, P. S. Baran, *Acc. Chem. Res.* **2012**, *45*, 826–839.
- [2] a) I. G. Denisov, T. M. Makris, S. G. Sligar, I. Schlichting, *Chem. Rev.* **2005**, *105*, 2253–2277; b) P. R. Ortiz de Montellano, *Chem. Rev.* **2010**, *110*, 932–948; c) S. Shaik, S. Cohen, Y. Wang, H. Chen, D. Kumar, W. Thiel, *Chem. Rev.* **2010**, *110*, 949–1017.
- [3] a) A. Glieder, E. T. Farinas, F. H. Arnold, *Nat. Biotechnol.* **2002**, *20*, 1135–1139; b) F. Xu, S. G. Bell, J. Lednik, A. Insley, Z. Rao, L. L. Wong, *Angew. Chem. Int. Ed.* **2005**, *44*, 4029–4032; *Angew. Chem.* **2005**, *117*, 4097–4100; c) M. Landwehr, L. Hochrein, C. R. Otey, A. Kasrayan, J.-E. Bäckvall, F. H. Arnold, *J. Am. Chem. Soc.* **2006**, *128*, 6058–6059; d) R. Fasan, M. M. Chen, N. C. Crook, F. H. Arnold, *Angew. Chem. Int. Ed.* **2007**, *46*, 8414–8418; *Angew. Chem.* **2007**, *119*, 8566–8570; e) S. Li, M. R. Chaulagain, A. R. Knauff, L. M. Podust, J. Montgomery, D. H. Sherman, *Proc. Natl. Acad. Sci. USA* **2009**, *106*, 18463–18468; f) A. Rentmeister, F. H. Arnold, R. Fasan, *Nat. Chem. Biol.* **2009**, *5*, 26–28; g) A. Robin, G. A. Roberts, J. Kisch, F. Sabbadin, G. Grogan, N. Bruce, N. J. Turner, S. L. Flitsch, *Chem. Commun.* **2009**, 2478–2480; h) J. C. Lewis, S. M. Mantovani, Y. Fu, C. D. Snow, R. S. Komor, C. H. Wong, F. H. Arnold, *ChemBioChem* **2010**, *11*, 2502–2505; i) E. Weber, A. Seifert, M. Antonovici, C. Geinitz, J. Pleiss, V. B. Urlacher, *Chem. Commun.* **2011**, *47*, 944–946; j) M. Bordeaux, A. Galarneau, F. Fajula, J. Drone, *Angew. Chem. Int. Ed.* **2011**, *50*, 2075–2079; *Angew. Chem.* **2011**, *123*, 2123–2127; k) S. Kille, F. E. Zilly, J. P. Acevedo, M. T. Reetz, *Nat. Chem.* **2011**, *3*, 738–743; l) V. Rea, A. J. Kolkman, E. Vottero, E. J. Stronks, K. A. Ampt, M. Honing, N. P. Vermeulen, S. S. Wijmenga, J. N. Commandeur, *Biochemistry* **2012**, *51*, 750–760; m) K. D. Zhang, B. M. Shafer, M. D. Demars, H. A. Stern, R. Fasan, *J. Am. Chem. Soc.* **2012**, *134*, 18695–18704; n) M. Bordeaux, A. Galarneau, J. Drone, *Angew. Chem. Int. Ed.* **2012**, *51*, 10712–10723; *Angew. Chem.* **2012**, *124*, 10870–10881.
- [4] L. M. Podust, D. H. Sherman, *Nat. Prod. Rep.* **2012**, *29*, 1251–1266.
- [5] R. Fasan, *ACS Catal.* **2012**, *2*, 647–666.
- [6] B. M. A. van Vugt-Lussenburg, E. Stjernschantz, J. Lastdrager, C. Oostenbrink, N. P. E. Vermeulen, J. N. M. Commandeur, *J. Med. Chem.* **2007**, *50*, 455–461.
- [7] J. N. Kolev, K. M. O'Dwyer, C. T. Jordan, R. Fasan, *ACS Chem. Biol.* **2014**, *9*, 164–173.
- [8] R. Fasan, Y. T. Meharena, C. D. Snow, T. L. Poulos, F. H. Arnold, *J. Mol. Biol.* **2008**, *383*, 1069–1080.
- [9] a) C. C. Liu, P. G. Schultz, *Annu. Rev. Biochem.* **2010**, *79*, 413–444; b) J. A. Johnson, Y. Y. Lu, J. A. Van Deventer, D. A. Tirrell, *Curr. Opin. Chem. Biol.* **2010**, *14*, 774–780.
- [10] a) M. R. Seyedsayamdost, J. Xie, C. T. Chan, P. G. Schultz, J. Stubbe, *J. Am. Chem. Soc.* **2007**, *129*, 15060–15071; b) J. C. Jackson, J. T. Hammill, R. A. Mehl, *J. Am. Chem. Soc.* **2007**, *129*, 1160–1166.
- [11] a) N. Wu, A. Deiters, T. A. Cropp, D. King, P. G. Schultz, *J. Am. Chem. Soc.* **2004**, *126*, 14306–14307; b) A. Deiters, D. Groff, Y. Ryu, J. Xie, P. G. Schultz, *Angew. Chem. Int. Ed.* **2006**, *45*, 2728–2731; *Angew. Chem.*

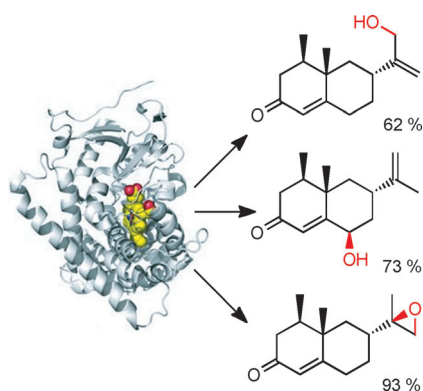
- 2006, 118, 2794–2797; c) D. Groff, M. C. Thielges, S. Cellitti, P. G. Schultz, F. E. Romesberg, *Angew. Chem. Int. Ed.* **2009**, *48*, 3478–3481; *Angew. Chem.* **2009**, *121*, 3530–3533.
- [12] a) J. N. Lampe, S. N. Floor, J. D. Gross, C. R. Nishida, Y. Jiang, M. J. Trnka, P. R. Ortiz de Montellano, *J. Am. Chem. Soc.* **2008**, *130*, 16168–16169; b) J. N. Lampe, R. Brandman, S. Sivaramakrishnan, P. R. de Montellano, *J. Biol. Chem.* **2010**, *285*, 9594–9603.
- [13] C. Aldag, I. A. Gromov, I. Garcia-Rubio, K. von Koenig, I. Schlichting, B. Jaun, D. Hilvert, *Proc. Natl. Acad. Sci. USA* **2009**, *106*, 5481–5486.
- [14] Y. Kimata, H. Shimada, T. Hirose, Y. Ishimura, *Biochem. Biophys. Res. Commun.* **1995**, *208*, 96–102.
- [15] a) J. C. Jackson, S. P. Duffy, K. R. Hess, R. A. Mehl, *J. Am. Chem. Soc.* **2006**, *128*, 11124–11127; b) I. N. Ugwumba, K. Ozawa, Z. Q. Xu, F. Ely, J. L. Foo, A. J. Herlt, C. Coppin, S. Brown, M. C. Taylor, D. L. Ollis, L. N. Mander, G. Schenk, N. E. Dixon, G. Otting, J. G. Oakeshott, C. J. Jackson, *J. Am. Chem. Soc.* **2011**, *133*, 326–333.
- [16] P. C. Cirino, Y. Tang, K. Takahashi, D. A. Tirrell, F. H. Arnold, *Biotechnol. Bioeng.* **2003**, *83*, 729–734.
- [17] L. O. Narhi, A. J. Fulco, *J. Biol. Chem.* **1987**, *262*, 6683–6690.
- [18] C. J. Whitehouse, S. G. Bell, L. L. Wong, *Chem. Soc. Rev.* **2012**, *41*, 1218–1260.
- [19] A. W. Munro, D. G. Leys, K. J. McLean, K. R. Marshall, T. W. Ost, S. Daff, C. S. Miles, S. K. Chapman, D. A. Lysek, C. C. Moser, C. C. Page, P. L. Dutton, *Trends Biochem. Sci.* **2002**, *27*, 250–257.
- [20] S. W. Santoro, L. Wang, B. Herberich, D. S. King, P. G. Schultz, *Nat. Biotechnol.* **2002**, *20*, 1044–1048.
- [21] L. Wang, Z. Zhang, A. Brock, P. G. Schultz, *Proc. Natl. Acad. Sci. USA* **2003**, *100*, 56–61.
- [22] A. L. Stokes, S. J. Miyake-Stoner, J. C. Peeler, D. P. Nguyen, R. P. Hammer, R. A. Mehl, *Mol. Biosyst.* **2009**, *5*, 1032–1038.
- [23] L. Wang, A. Brock, P. G. Schultz, *J. Am. Chem. Soc.* **2002**, *124*, 1836–1837.
- [24] a) G. McLendon, E. Radany, *J. Biol. Chem.* **1978**, *253*, 6335–6337; b) D. A. Parsell, R. T. Sauer, *J. Biol. Chem.* **1989**, *264*, 7590–7595; c) I. Inoue, M. Rechsteiner, *J. Biol. Chem.* **1994**, *269*, 29241–29246.
- [25] A. Gliszczynska, A. Lysek, T. Janeczko, M. Switalska, J. Wietrzyk, C. Wawrzenczyk, *Bioorg. Med. Chem.* **2011**, *19*, 2464–2469.
- [26] M. J. McLachlan, T. W. Johannes, H. Zhao, *Biotechnol. Bioeng.* **2008**, *99*, 268–274.
- [27] W. C. Huang, A. C. Westlake, J. D. Marechal, M. G. Joyce, P. C. Moody, G. C. Roberts, *J. Mol. Biol.* **2007**, *373*, 633–651.
- [28] S. Kadkhodayan, E. D. Coulter, D. M. Maryniak, T. A. Bryson, J. H. Dawson, *J. Biol. Chem.* **1995**, *270*, 28042–28048.
- [29] K. Zhang, S. El Damaty, R. Fasan, *J. Am. Chem. Soc.* **2011**, *133*, 3242–3245.
- [30] M. Satyanarayana, F. Vitali, J. R. Frost, R. Fasan, *Chem. Commun.* **2012**, *48*, 1461–1463.
- [31] R. J. Sowden, S. Yasmin, N. H. Rees, S. G. Bell, L. L. Wong, *Org. Biomol. Chem.* **2005**, *3*, 57–64.

Received: January 25, 2014

Published online on ■ ■ ■, 0000

FULL PAPERS

Unnatural choice: Incorporating unnatural amino acids at single positions within the active site of a cytochrome P450 significantly changes the regioselectivity (shown) of the enzyme or enhances its catalytic efficiency. This study demonstrates that unnatural amino acid mutagenesis constitutes a promising new strategy for improving P450 oxidation catalysts.



*J. N. Kolev, J. M. Zaengle, R. Ravikumar, R. Fasan**



Enhancing the Efficiency and Regioselectivity of P450 Oxidation Catalysts by Unnatural Amino Acid Mutagenesis



CHEMBIOCHEM

Supporting Information

© Copyright Wiley-VCH Verlag GmbH & Co. KGaA, 69451 Weinheim, 2014

Enhancing the Efficiency and Regioselectivity of P450 Oxidation Catalysts by Unnatural Amino Acid Mutagenesis

Joshua N. Kolev, Jacqueline M. Zaengle, Rajesh Ravikumar, and Rudi Fasan^{*[a]}

cbic_201400060_sm_miscellaneous_information.pdf

Table S1. Sequence of the oligonucleotides used for the preparation of the uP450 variants.

Primer	Sequence
A74tag_for	GATAAAAACCTTAAGTCAATAGCTTAAATTC
A74tag_rev	GAATTTAAGCTATTGACTTAAGTTTTTATC
L75tag(78A)_for	GATAAAAACCTTAAGTCAAGCGTAGAAATTCG
L75tag(78A)_rev	CGAATTTCTACGCTTGACTTAAGTTTTTATC
V78tag_for	GTCAAGCGCTTAAATTCTAGCGTGATTTT
V78tag_rev	AAAATCACGCTAGAATTTAAGCGCTTGAC
F81tag_for	CGTGATTAGGCAGGAGACGGG
F81tag_rev	CCCGTCTCCTGCCTAATCACG
A82tag_for	CGTGATTTTTAGGGAGACGGGTTA
A82tag_rev	TAACCCGTCTCCCTAAAATCACG
F87tag_fwd	GACGGGTTATAGACAAGCTGGACG
F87tag_rev	CGTCCAGCTTGCTCTATAACCCGTC
L181tag(184V)_for	CGTGCATAGGATGAAGTAATGAACAAGC
L181tag(184V)_rev	GCTTGTTCACTTTCATCCTATGCACG
A184tag_for	GCACTGGATGAATAGATGAACAAG
A184tag_rev	CTTGTTTCATCTATTCATCCAGTGC
L188tag_for	GAACAAGTAGCAGCGAGCAAATCC
L188tag_rev	GGATTTGCTCGCTGCTACTTGTTTC
T327tag_for	GGCCATAGGCTCCTGCGTTTTCC
T327tag_rev	GGAAAACGCAGGAGCCTATGGCC
A328tag_for	GGCCAACCTTAGCCTGCGTTTTCC
A328tag_rev	GGAAAACGCAGGCTAAGTTGGCC

Table S2. Product distribution for the oxidation of (*S*)-ibuprofen ME (**1**) and (+)-nootkatone (**2**) by the uP450 variants. Highlighted in green and blue are the P450 variants whose site-selectivity differs more than 30% and more than 50%, respectively, from the parent enzyme (139-3 variant). NA= not active.

Position	UAA	(S)-ibuprofen (1)		Nootkatone (2)		
		3	4	5	6	7
Parent P450		62%	38%	96%	4%	0
74	OBnY	55%	45%	94%	6%	0%
75	OBnY	25%	75%	89%	11%	0%
78	OBnY	65%	35%	64%	0%	36%
81	OBnY	71%	29%	88%	6%	6%
82	OBnY	67%	33%	57%	22%	21%
87	OBnY	52%	48%	77%	5%	18%
181	OBnY	15%	85%	93%	7%	0%
184	OBnY	49%	51%	91%	9%	0%
188	OBnY	59%	41%	96%	4%	0%
327	OBnY	58%	42%	NA	NA	NA
328	OBnY	22%	78%	92%	8%	0%
74	pAcF	56%	44%	95%	5%	0%
75	pAcF	22%	78%	95%	5%	0%
78	pAcF	87%	13%	32%	0%	68%
81	pAcF	55%	45%	97%	3%	0%
82	pAcF	72%	28%	38%	62%	0%
87	pAcF	53%	47%	95%	5%	0%
181	pAcF	30%	70%	79%	4%	17%
184	pAcF	31%	69%	94%	6%	0%
188	pAcF	58%	42%	96%	4%	0%
327	pAcF	63%	37%	95%	5%	0%
328	pAcF	0%	100%	88%	12%	0%
74	pAmF	38%	62%	94%	6%	0%
75	pAmF	18%	82%	94%	6%	0%
78	pAmF	68%	32%	91%	9%	0%
81	pAmF	39%	61%	92%	8%	0%
82	pAmF	73%	27%	79%	21%	0%
87	pAmF	60%	40%	95%	5%	0%
181	pAmF	60%	40%	96%	4%	0%
184	pAmF	50%	50%	97%	3%	0%
188	pAmF	69%	31%	96%	4%	0%

327	<i>pAmF</i>	65%	35%	95%	5%	0%
328	<i>pAmF</i>	NA	NA	93%	7%	0%
74	NapA	64%	36%	95%	5%	0%
75	NapA	47%	53%	94%	6%	0%
78	NapA	79%	21%	79%	6%	15%
81	NapA	57%	43%	86%	5%	9%
82	NapA	78%	22%	51%	41%	8%
87	NapA	NA	NA	90%	10%	0%
181	NapA	53%	47%	81%	4%	15%
184	NapA	28%	72%	87%	8%	5%
188	NapA	63%	37%	96%	4%	0%
327	NapA	59%	41%	96%	4%	0%
328	NapA	0%	100%	75%	25%	0%

Figure S1. UAA incorporation efficiency of the aaRSs. Relative fluorescence intensity as dependent upon the relative expression level of the YFP(amber stop) reporter protein in the presence of the different aaRSs (and cognate unnatural amino acids) investigated in this study.

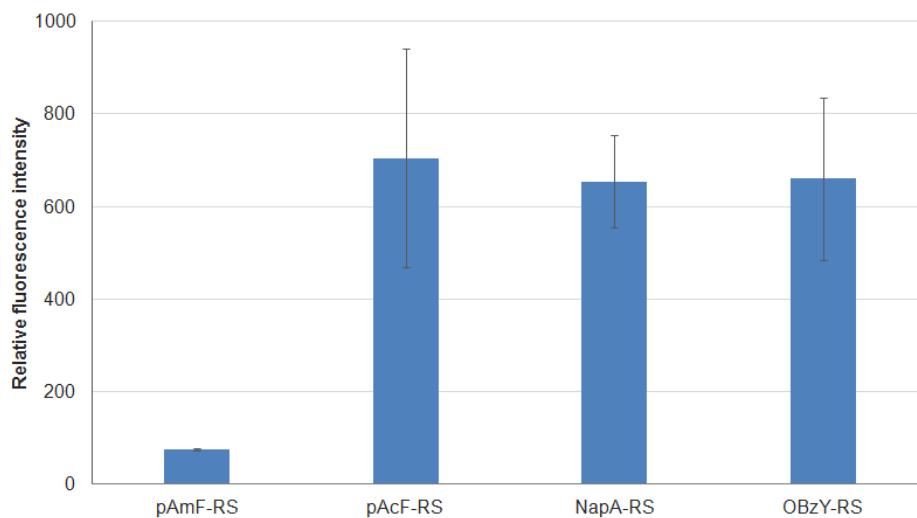


Figure S2. Heme spin shift experiments with the tyrosine-substituted P450 variants. A) Electronic absorption spectrum before (black line) and after (red line) addition of saturating concentration (0.5 mM) of (+)-nootkatone (**2**). B) Plot of substrate-induced heme spin shift at varying (+)-nootkatone (**2**) concentration. The experimental data (dots) are fitted to a non-cooperative 1:1 binding model equation (solid line). The calculated equilibrium dissociation constant (K_D) is indicated.

